ESTIMATION OF VISUAL EVOKED POTENTIALS FOR MEASUREMENT OF OPTICAL PATHWAY CONDUCTION

Mohd Zuki Yusoff, Nidal Kamel

Electrical & Electronic Engineering Department, University Teknologi PETRONAS
Bandar Seri Iskandar, 31750 Tronoh, Perak, MALAYSIA
phone: + (605) 368 7807, fax: + (605) 365 7443, email: mzuki_yusoff@petronas.com.my
web: http://www.utp.edu.my

ABSTRACT

A time domain constrained subspace-based estimator for extracting a visual evoked potential (VEP) from a highly noisy brain activity is proposed. Generally, the desired VEP is corrupted by background electroencephalogram (EEG) behaving as colored noise, making the overall signal-to-noise ratio as low as -10 dB. The estimator is designed to minimize signal distortion, while keeping residual noise below a specified threshold. Also, the algorithm applies a Karhunen-Loeve transform to decorrelate the corrupted VEP signal and decompose it into two parts called signal and noise subspace. Before an inverse Karhunen-Loeve transform is applied, the noise only subspace is discarded. VEP enhancement is therefore achieved by estimating the desired VEP only from the signal subspace. The performance of the filter to detect the latencies of P100's is comprehensively assessed using realistically simulated VEP and EEG data. Later, the effectiveness and validity of the algorithm are evaluated using real patient data recorded in a clinical environment. The results from both experiments show that the estimator generates reasonably low errors and high success rate.

Keywords: *Eigenvalue decomposition, subspace methods, time-domain estimator, visual evoked potentials.*

1. INTRODUCTION

Visual evoked potentials (VEPs) are special types of elecroencephalogram (EEG) signals generated by the human brain when a specific visual stimulation is applied to the eye (left or right) of the subject under study. In a hospital, a visual evoked potential test remains as the only **objective test** [1] to assess the physiology (i.e., conduction) of the visual or optical pathway from the retina to the occipital cortex of the brain. Primarily, the latency of the robust and positive going P100 component is used by clinicians to check the integrity of the visual pathways. For normal subjects, their P100 components usually produce latencies very close to 100 ms. On the contrary, subjects with defective visual pathways will register prolonged P100 latencies (e.g., at 120 ms, 130 ms, etc.). As an example, a doctor uses the P100 reading as one of the decision making factors whether or not a cornea transplant can be performed on a patient.

In comparison to the frequencies of the ongoing EEGs, VEPs are dominated by a lower frequency spectrum. Nonetheless, significant amount of EEG frequencies with much higher power reside in the same band as that of the VEPs. Practically, due to very poor signal-to-noise ratio (SNR) at -5 to -10 dB, the true VEP forms are not readily available from brain recordings since they are highly mixed with the spontaneous EEG waves, which can be regarded as colored noise. As such, the estimation of VEP from background brain activities still poses a great but an interesting challenge to signal processing researchers.

This paper is an extension of our signal subspace work reported in [2]. It provides more comprehensive theoretical information, statistically larger experimental data and therefore reliable test results involving both simulated and real patient data. Another variation of our subspace approach is documented in [3].

The focus of this study is to correctly estimate VEP latencies, instead of VEP amplitudes; doctors are normally interested in the VEP latencies as opposed to the VEP amplitudes, as far as the VEP test is concerned. The VEP extraction method presented here is inspired by work from a speech enhancement area, originally proposed by Ephraim and Van Trees [4] for white noise elimination, and further extended by Rezayee and Gazor [5] to deal with colored noise. In this paper, we apply the constrained optimization concept suggested by [4] and adapt the estimator enhanced by [5] to estimate the P100 components from EEG background, without using a pre-whitening stage.

2. MODEL DEVELOPMENT

2.1 VEP Model

It is assumed that a VEP is actually a “known" waveform which can be artificially produced. The created VEP will then be added to much higher power “colored noise” that represents EEG and other background noise. The resultant waveform will be treated as a composite signal that needs to be processed and extracted using the developed technique to get back the desired VEP. Thus, the following model is defined.

$$\boldsymbol{y} = \boldsymbol{x} + \boldsymbol{n} \tag{1}$$

where, $\boldsymbol{y}$ is the M-dimensional vector of the corrupted (noisy) VEP signal; $\boldsymbol{x}$ is the M-dimensional vector of the original (clean) VEP signal; $\boldsymbol{n}$ is the M-dimensional vector of the additive EEG noise which is assumed to be uncorrelated with $\boldsymbol{x}$. Further, $\boldsymbol{H}$ is defined as the M x M-dimensional matrix of the VEP time-domain constrained linear estimator.

Next, $\hat{\boldsymbol{x}}$ is defined as the M-dimensional vector of the estimated VEP signal. The estimated VEP signal $\hat{\boldsymbol{x}}$ is related to $\boldsymbol{H}$ and $\boldsymbol{y}$ in the following way:

$$\hat{\boldsymbol{x}} = \boldsymbol{H}.\boldsymbol{y} \tag{2}$$

The estimated VEP signal $\hat{\boldsymbol{x}}$ will never be exactly equal to the original VEP signal $\boldsymbol{x}$; the error signal $\boldsymbol{\varepsilon}$ defined by [4] is written as:

$$\begin{aligned}\boldsymbol{\varepsilon} &= \hat{\boldsymbol{x}} - \boldsymbol{x} = \boldsymbol{H}\boldsymbol{y} - \boldsymbol{x} = (\boldsymbol{H} - \boldsymbol{I})\boldsymbol{x} + \boldsymbol{H}\boldsymbol{n} \\ &= \boldsymbol{\varepsilon}_x + \boldsymbol{\varepsilon}_n \quad \text{where } \boldsymbol{\varepsilon}_x = (\boldsymbol{H} - \boldsymbol{I})\boldsymbol{x}, \quad \boldsymbol{\varepsilon}_n = \boldsymbol{H}\boldsymbol{n}\end{aligned} \tag{3}$$

The $\boldsymbol{\varepsilon}_x$ represents the VEP distortion and $\boldsymbol{\varepsilon}_n$ represents the residual noise. If the VEP signal covariance matrix $\boldsymbol{R}_x$ is known, then the energies of the signal distortion can be written as

$$\bar{\boldsymbol{\varepsilon}}_x^2 = \mathrm{tr}\left(\mathrm{E}\left\{\boldsymbol{\varepsilon}_x \boldsymbol{\varepsilon}_x^T\right\}\right) = \mathrm{tr}\left((\boldsymbol{H} - \boldsymbol{I})\boldsymbol{R}_x(\boldsymbol{H} - \boldsymbol{I})^T\right) \tag{4}$$

Similarly, if the EEG noise covariance matrix $\boldsymbol{R}_n$ is known, the energies of the residual noise can be expressed as

$$\bar{\boldsymbol{\varepsilon}}_n^2 = \mathrm{tr}\left(\mathrm{E}\left\{\boldsymbol{\varepsilon}_n \boldsymbol{\varepsilon}_n^T\right\}\right) = \mathrm{tr}\left(\boldsymbol{H}\boldsymbol{R}_n\boldsymbol{H}^T\right) \tag{5}$$

Both energies in (4) and (5) lead to the total residual energies given as

$$\bar{\boldsymbol{\varepsilon}}^2 = \bar{\boldsymbol{\varepsilon}}_x^2 + \bar{\boldsymbol{\varepsilon}}_n^2 \tag{6}$$

The EEG noise covariance matrix $\boldsymbol{R}_n$ can be obtained from the pre-stimulation EEG samples, during which the VEP signals are absent. If the VEP and EEG noise are independent, the following relationships can be established:

$$\boldsymbol{R}_y = \boldsymbol{R}_x + \boldsymbol{R}_n \tag{7}$$

where, $\boldsymbol{R}_y$ is the covariance matrix of the corrupted VEP. Using (7), we can calculate $\boldsymbol{R}_x$ by subtracting $\boldsymbol{R}_n$ from $\boldsymbol{R}_y$.

The aim is to minimize the unwanted energies in (6) so that the generated error is minimal. A difficulty arises since lowering noise energies means increasing the distortion energies, and vice versa. Therefore, a proper balance needs to be determined so that the noise residues can be reasonably reduced without introducing significant distortion to the processed signal. The excessive amount of the residual noise prohibits the discrimination between the desired VEP peak (i.e., the P100) and the noise peaks itself, even if the desired signal is successfully extracted. On the other hand, the excessive distortion means the desired VEP peak may have shifted either to the left or right of its original position, resulting in an inaccurate measurement of the VEP latency.

2.2 Estimator Optimization

An optimal time domain constrained linear estimator $\boldsymbol{H}$ that minimizes the VEP signal distortion and maintains the residual noise within a permissible level, is mathematically formulated by [4] as

$$\boldsymbol{H}_{opt} = \min_{\boldsymbol{H}} \ \bar{\boldsymbol{\varepsilon}}_x^2 \ \text{ subject to} : \bar{\boldsymbol{\varepsilon}}_n^2 \leq M\sigma^2 \tag{8}$$

where M is the dimension of the noisy vector space and σ^2 is a positive constant noise threshold level. The σ^2 in (8) dictates the amount of the residual noise allowed to remain in the linear estimator. Next, the Lagrangian function in association with the "Kuhn-Tucker necessary conditions for constrained minimization" [4] are applied to (8) to obtain $\boldsymbol{H}_{opt}$. The formed Lagrangian function can be expressed as

$$\boldsymbol{L}(\boldsymbol{H}, \mu) = \bar{\boldsymbol{\varepsilon}}_x^2 + \mu(\bar{\boldsymbol{\varepsilon}}_n^2 - M\sigma^2) \tag{9}$$

where μ is the Lagrange multiplier. It follows that the filter matrix $\boldsymbol{H}$ is a stationary feasible point if it satisfies the following gradient equation $\nabla_H \boldsymbol{L}(\boldsymbol{H}, \mu) = 0$:

$$\frac{\partial \boldsymbol{L}(\boldsymbol{H}, \mu)}{\partial \boldsymbol{H}} = \frac{\partial}{\partial \boldsymbol{H}}[\bar{\boldsymbol{\varepsilon}}_x^2 + \mu(\bar{\boldsymbol{\varepsilon}}_n^2 - M\sigma^2)] = 0 \tag{10}$$

Subsequently, the gradient equation in (10) can be solved to yield $\boldsymbol{H}$.

$$\begin{aligned}&\frac{\partial}{\partial \boldsymbol{H}}[\mathrm{tr}\left((\boldsymbol{H} - \boldsymbol{I})\boldsymbol{R}_x(\boldsymbol{H} - \boldsymbol{I})^T\right)] + \frac{\partial}{\partial \boldsymbol{H}}[\mu \mathrm{tr}\left(\boldsymbol{H}\boldsymbol{R}_n\boldsymbol{H}^T\right)] = 0 \\ &2(\boldsymbol{H} - \boldsymbol{I})\boldsymbol{R}_x + 2\mu\boldsymbol{H}\boldsymbol{R}_n - 0 = 0 \\ &\Rightarrow \boldsymbol{H} = \boldsymbol{R}_x(\boldsymbol{R}_x + \mu\boldsymbol{R}_n)^{-1}\end{aligned} \tag{11}$$

The filter matrix $\boldsymbol{H}$ stated in (11) functions as a fixed filter, which performs well to estimate the VEP at a relatively high SNR. As the SNR degrades, it is desirable if $\boldsymbol{H}$ can be adjusted and manipulated accordingly to minimize the noise residues while keeping the signal distortion at an acceptable level.

2.3 Karhunen-Loeve Transform

The Karhunen-Loeve Transform (KLT) is a unitary linear transform widely applied in signal processing areas. The KLT scheme exploits the statistical properties of a discrete-time stochastic process; KLT optimally decorrelates the process by means of diagonalizing its correlation matrix.

Theorem 1 (Karhunen-Loeve Transform). Let $\boldsymbol{R}_a$ be the MxM symmetric correlation matrix of a discrete-time stochastic process $a(n)$. Further, let $\boldsymbol{V}$ and $\boldsymbol{D}$ be the corresponding MxM unitary eigenvector and eigenvalue matrices of $\boldsymbol{R}_a$. Then KLT is defined as the unitary transform of the following form:

$$\boldsymbol{R}_a = \boldsymbol{V}\boldsymbol{D}\boldsymbol{V}^{-1} = \boldsymbol{V}\boldsymbol{D}\boldsymbol{V}^T, \ \boldsymbol{V}^{-1} = \boldsymbol{V}^T \text{ for unitary } \boldsymbol{V} \tag{12}$$

The relationships among various parameters established in (12) can be achieved by taking eigendecomposition on $\boldsymbol{R}_a$. It follows that (12) can be rearranged accordingly to compute the diagonal eigenvalue $\boldsymbol{D} = \mathrm{diag}\,[d_1, d_2, ..., d_M]$; that is

$$\boldsymbol{D} = \boldsymbol{V}^{-1}\boldsymbol{R}_a\boldsymbol{V}^{-T} = \boldsymbol{V}^T\boldsymbol{R}_a\mathrm{V}, \ \boldsymbol{V}^{-T} = \boldsymbol{V} \text{ for unitary } \boldsymbol{V} \tag{13}$$

Equation (13) reveals that $\boldsymbol{R}_a$ is transformed by the $\boldsymbol{V}^T$ (i.e., KLT matrix) and $\boldsymbol{V}$ (i.e., inverse KLT) terms into the diagonal matrix $\boldsymbol{D}$, resulting in the optimal decorrelation of the stochastic process.

Proof: The KLT and IKLT concept involving a column vector $\boldsymbol{a}$ and its correlation matrix $\boldsymbol{R}_a$, is represented by a block diagram shown in Figure 1 below.

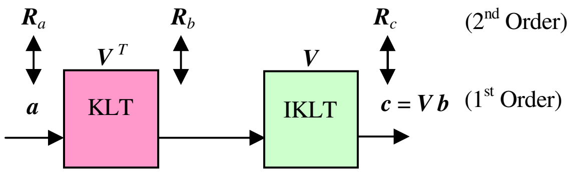

Figure 1 - KLT and IKLT schemes involving an original vector **a** and a unitary eigenvector ***V***.

With reference to Figure 1, let $\boldsymbol{b}$ represent a column vector after the KLT of $\boldsymbol{a}$, and let $\boldsymbol{c}$ represent a column vector after the IKLT block. The transformation of $\boldsymbol{a}$ into $\boldsymbol{b}$ is achieved using the KLT matrix $\boldsymbol{V}^T$.

$$\boldsymbol{b} = \boldsymbol{V}^{-1}\boldsymbol{a} = \boldsymbol{V}^T\boldsymbol{a} \qquad (14)$$

To obtain decorrelation, the correlation matrix of $\boldsymbol{b}$ is computed as the expectation of the outer product of $\boldsymbol{b}$ by itself, written as

$$\boldsymbol{R}_b = \mathrm{E}\{\boldsymbol{b}\boldsymbol{b}^T\} = \mathrm{E}\{\boldsymbol{V}^T\boldsymbol{a}(\boldsymbol{V}^T\boldsymbol{a})^T\} = \boldsymbol{V}^T\boldsymbol{R}_a\boldsymbol{V} = \boldsymbol{D} \qquad (15)$$

The matrix $\boldsymbol{R}_a$ is linearly transformed into $\boldsymbol{R}_b$ by the $\boldsymbol{V}^T\boldsymbol{R}_a\boldsymbol{V}$ term; the correlation matrix $\boldsymbol{R}_b$ of $\boldsymbol{b}$ is actually the eigenvalue matrix $\boldsymbol{D}$ of $\boldsymbol{R}_{\mathrm{a}}$. Since $\boldsymbol{R}_b$ is fully diagonal, it can be concluded that the cross-correlation has been removed. In order to return to the original space before the transform in the KLT domain, the inverse transform using the IKLT matrix $\boldsymbol{V}$ needs to be performed on $\boldsymbol{b}$; that is,

$$\boldsymbol{c} = \boldsymbol{V}\boldsymbol{b} = \boldsymbol{V}\boldsymbol{V}^T\boldsymbol{a} = \boldsymbol{a} \qquad (16)$$

From (16), it is clear that the original vector $\boldsymbol{a}$ has been recovered. Furthermore, the correlation matrix of $\boldsymbol{c}$ is computed as the expectation of the outer product of $\boldsymbol{c}$ by itself, written as

$$\begin{aligned}\boldsymbol{R}_c &= \mathrm{E}\{\boldsymbol{c}\boldsymbol{c}^T\} = \mathrm{E}\{\boldsymbol{V}\boldsymbol{b}(\boldsymbol{V}\boldsymbol{b})^T\} = \boldsymbol{V}\boldsymbol{R}_b\boldsymbol{V}^T \\ &= \boldsymbol{V}\boldsymbol{V}^T\boldsymbol{R}_a\boldsymbol{V}\boldsymbol{V}^T = \boldsymbol{R}_a \quad \text{where } \boldsymbol{R}_b = \boldsymbol{V}^T\boldsymbol{R}_a\boldsymbol{V}\end{aligned} \qquad (17)$$

From (17), it is clear that the correlation matrix $\boldsymbol{R}_a$ has been recovered by taking the linear inverse transform of $\boldsymbol{R}_b$ denoted by the $\boldsymbol{V}\boldsymbol{R}_b\boldsymbol{V}^T$ term. Alternatively, the KLT expansion is termed as a *subspace estimator* when some of the decomposed orthogonal components are truncated to reject noise. The truncation means some eigenvalues and corresponding eigenvectors carrying unwanted elements are removed; only the components deemed to be significant are retained in the process. The reduced matrix is then reconstructed to estimate the required signal. In brief, the decomposition and decorrelation of a noisy observation can be performed using eigenvalue decomposition (EVD).

2.4 Generic Subspace Approach

With reference to (11), eigenvalue decomposition is to be performed on $\boldsymbol{R}_x$ and $\boldsymbol{R}_n$. By assuming that $\boldsymbol{R}_x = \boldsymbol{U}\boldsymbol{\Delta}_x\boldsymbol{U}^T$ and $\boldsymbol{R}_n = \boldsymbol{U}\boldsymbol{\Delta}_n\boldsymbol{U}^T$ exist, we rewrite (11) as

$$\boldsymbol{H}_{opt} = \boldsymbol{U}\boldsymbol{\Delta}_x(\boldsymbol{\Delta}_x + \mu\boldsymbol{\Delta}_n)^{-1}\boldsymbol{U}^T \qquad (18)$$

where, $\boldsymbol{H}_{opt}$ denotes an optimal estimator; $\boldsymbol{U}$ is the unitary eigenvector matrix produced from a symmetric basis matrix $\boldsymbol{\Sigma}$ which is to be computed from the proper combinations of $\boldsymbol{R}_x$ and $\boldsymbol{R}_n$ terms; $\boldsymbol{\Delta}_x$ is the diagonal eigenvalue matrix of $\boldsymbol{R}_x$; $\boldsymbol{\Delta}_n$ is the diagonal eigenvalue matrix of $\boldsymbol{R}_n$; μ is the Lagrange multiplier which has to be set to a proper value. The higher value of μ eliminates more noise residues at the expense of higher distortion in the recovered VEP.

Theoretically, the linear estimator in (18) functions optimally if the unitary eigenvector matrix $\boldsymbol{U}$ derived from $\boldsymbol{\Sigma}$ is able to simultaneously diagonalize both $\boldsymbol{R}_x$ and $\boldsymbol{R}_n$. The full diagonalization of their eigenvalues can be obtained if and only if $\boldsymbol{R}_x$ and $\boldsymbol{R}_n$ multiplication is commutative (i.e., $\boldsymbol{R}_x\boldsymbol{R}_n = \boldsymbol{R}_n\boldsymbol{R}_x$). In reality, complete diagonalization (i.e., without pre-whitening) is not possible since their multiplication is non-commutative.

2.5 Signal Subspace Method Based on the Covariance Matrix of the Observed Signal

Next, we assume that $\boldsymbol{\Sigma} = \boldsymbol{R}_y$ produces an eigenvector matrix that shall approximately diagonalize both $\boldsymbol{R}_x$ and $\boldsymbol{R}_n$. This choice of $\boldsymbol{\Sigma}$ is the same as that used by [5]. The eigenvalue matrices of the desired VEP and the unwanted noise are then calculated as follows:

$$\boldsymbol{\Lambda}_x \equiv E[\boldsymbol{U}^T\boldsymbol{x}\,\boldsymbol{x}^T\boldsymbol{U}] = \boldsymbol{U}^T\boldsymbol{R}_x\boldsymbol{U} \approx \boldsymbol{V}^T\boldsymbol{R}_x\boldsymbol{V} \qquad (19)$$

$$\boldsymbol{\Lambda}_n \equiv E[\boldsymbol{U}^T\boldsymbol{n}\,\boldsymbol{n}^T\boldsymbol{U}] = \boldsymbol{U}^T\boldsymbol{R}_n\boldsymbol{U} \approx \boldsymbol{V}^T\boldsymbol{R}_n\boldsymbol{V} \qquad (20)$$

Applying (19) and (20) to (18), we approximate our signal subspace method (SSM) estimator as

$$\boldsymbol{H}_{SSM} = \boldsymbol{V}\boldsymbol{\Lambda}_x(\boldsymbol{\Lambda}_x + \mu\boldsymbol{\Lambda}_n)^{-1}\boldsymbol{V}^T = \boldsymbol{V}\boldsymbol{G}\boldsymbol{V}^T \qquad (21)$$

where $\boldsymbol{G} = \boldsymbol{\Lambda}_x(\boldsymbol{\Lambda}_x + \mu\boldsymbol{\Lambda}_n)^{-1}$ is known as the gain matrix.

The estimated VEP is then calculated as

$$\hat{\boldsymbol{x}}_{SSM} = \boldsymbol{H}_{SSM}\,.\,\mathbf{y} = \boldsymbol{V}\boldsymbol{G}\boldsymbol{V}^T.\,\mathbf{y} \qquad (22)$$

The corrupted VEP signal $\boldsymbol{y}$ in (22) is decorrelated by the KLT matrix $\boldsymbol{V}^T$. Then, the transformed signal is modified by a signal subspace gain matrix $\boldsymbol{G}$. Next, the modified signal is retransformed back into the original form by the inverse KLT matrix $\boldsymbol{V}$ to obtain the desired signal.

2.6 Algorithm Implementation

The proposed approach can be formulated in the following six steps. For each VEP trial:

Step 1: Compute the covariance matrix of the noisy signal $\boldsymbol{R}_y$, and the noise covariance matrix $\boldsymbol{R}_n$.

Step 2: Perform the eigendecomposition of $\boldsymbol{\Sigma} = \boldsymbol{R}_y$, extract the resulting eigenvector matrix $\boldsymbol{V}$, and compute the signal and EEG noise eigenvalue matrices $\boldsymbol{\Lambda}_x$ and $\boldsymbol{\Lambda}_n$, respectively.

Step 3: Assuming that λ_k series represented by $\lambda_1 > \lambda_2 > \lambda_3 \ldots \lambda_M$ are the diagonal elements of $\boldsymbol{\Lambda}_x$ sequenced in descending order, approximate the dimension L of the VEP signal subspace by counting the number of non-zero elements of $\boldsymbol{\Lambda}_x$.

$$L = \arg\{ \max_{1 \le k \le M} \lambda_k > 0 \} \tag{23}$$

Step 4: Compute the gain vector of the estimator as follows:

$$q(i) = \frac{\lambda_x(i)}{\lambda_x(i) + \mu\, \lambda_n(i)} \qquad 1 \le i \le L \tag{24}$$

Experimentally, μ was varied from 0 to 25, and μ = 2 was found to be ideal. The gain matrix $\boldsymbol{G}$ is obtained by diagonalizing the gain vector, $\boldsymbol{q}$.

$$\boldsymbol{G} = \begin{bmatrix} \mathrm{diag}\{q\} & 0 \\ 0 & 0 \end{bmatrix} = \begin{bmatrix} Q & 0 \\ 0 & 0 \end{bmatrix} \tag{25}$$

Step 5: Determine the linear SSM estimator $\boldsymbol{H}_{SSM}$ as follows:

$$\boldsymbol{H}_{SSM} = \boldsymbol{V} \cdot \boldsymbol{G} \cdot \boldsymbol{V}^T \tag{26}$$

Step 6: Estimate the enhanced VEP signal by:

$$\hat{\boldsymbol{x}}_{SSM} = \boldsymbol{H}_{SSM} \cdot \boldsymbol{y} \tag{27}$$

3. PERFORMANCE EVALUATION

The SSM method was tested and assessed using artificial and real human data.

3.1 Assessment of the Algorithm using Artificial Data

The clean artificial VEP $\boldsymbol{x}$ was generated by superimposing several Gaussian functions; the amplitudes, variance and mean of these functions were tweaked to generate precise peak latencies at 100 ms, mimicking the real P100.

The pre-stimulation EEG colored noise $\boldsymbol{n\_pre}$ was generated using an autoregressive (AR) model [6] governed by

$$\boldsymbol{v}(n) = 1.5084\boldsymbol{v}(n-1) - 0.1587\boldsymbol{v}(n-2) - 0.3109\boldsymbol{v}(n-3) - 0.0510\boldsymbol{v}(n-4) + \boldsymbol{u}(n) \tag{28}$$

The artificial post-stimulation EEG noise $\boldsymbol{n}$ was generated by changing the variance of $\boldsymbol{n\_pre}$. The artificially-corrupted VEP signal $\boldsymbol{y}$ was then produced by adding $\boldsymbol{x}$ and $\boldsymbol{n}$.

To test the robustness of SSM, the ratio of the artificial VEP over the EEG noise was varied from approximately +0 dB to -11dB. The corrupted VEP signal with a specific value of SNR was applied to the input of the SSM filter and the estimated P100 waveform was retrieved at the output. To obtain reliable statistics, five hundred different runs were performed for each level of SNR. Any trial was noted as a failure if the intended peak could not be differentiated from noise, or if the peak was totally absent. For successful runs, the values of the extracted peaks were precisely recorded. The highest peak in the waveform is considered as the wanted P100 component.

Next, the average errors e_{P100} in estimating the latency of the P100 was calculated as follows:

$$e_{P100} = \sum_{i=1}^{500} \left| \hat{t}_{P100} - 100 \right| \tag{29}$$

where $\hat{t}_{P100}$ represents the estimated P100 latency in milliseconds. Table 1 below tabulates the success rate and average errors for the SSM estimator.

Table 1 - The failure rate and average errors of the SSM estimator at SNR = 0 to -11 dB.

SNR [dB]	Failure Rate [%]	Average Error	SNR [dB]	Failure Rate [%]	Average Error
0	4.2	4.7	-6	13.6	6.5
-1	5.6	4.9	-7	14.4	7.2
-2	6.8	5.4	-8	16.2	8.0
-3	8.0	5.4	-9	17.2	8.3
-4	10.8	6.3	-10	17.4	8.8
-5	12.6	6.3	-11	18.3	9.4

From Table 1, it can be stated that SSM produces the least failure rate at 0 dB and the highest failure rate at -11 dB. Correspondingly, the lowest average error occurs at 0 dB and the highest one is generated at -11 dB also. In the worst case condition, SSM produces failure rate slightly less than 19 % and an average error slightly less than 10.

For some graphical illustrations, various waveforms with successfully estimated P100's at -6 and -11 dB are shown in Figure 2 below.

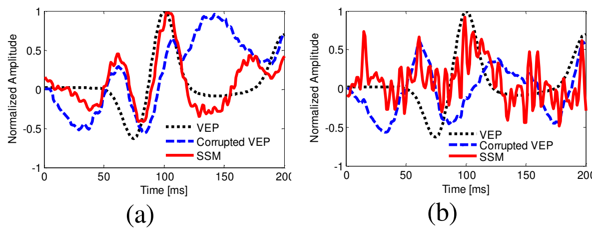

Figure 2 - Clean VEP, corrupted VEP and estimated VEP waveforms. (a) Estimation by SSM at -6 dB; (b) Estimation by SSM at -11 dB.

3.2 Assessment of the Algorithm using Human Data

This section reveals the accuracy of the SSM technique in estimating human P100 peaks, which are used by doctors as objective evaluation of the visual pathway conduction. Experiments were conducted at Selayang Hospital, Kuala Lumpur using RETIport32 equipment, and carried out on sixteen subjects having **normal** (P100 ≤ 115 ms) and **abnormal** (P100 > 115 ms) VEP readings. They were asked to watch a pattern reversal checkerboard pattern. The detailed test setup (sampling frequency, electrode connections, etc.) can be found in [3]. Eighty trials for each subject's right eye were processed by the VEP machine using ensemble averaging (EA). The averaged values were readily available and directly obtained from the equipment. Since EA is a multi-trial scheme, it is expected to produce good estimation of the P100 that can be used as a baseline for comparing the SSM estimator performance.

Further, SSM requires unprocessed data from the machine. Thus, the equipment was configured accordingly to generate the raw data. The recording for every trial involved capturing the brain activities for 333 ms before stimulation was applied; this enabled us to capture the colored EEG noise alone. The next 333 ms was used to record the post-stimulus EEG, comprising a mixture of the VEP and EEG. The same process was repeated for the consecutive trials. For comparisons with EA, the eighty different waveforms per subject produced by SSM were also averaged. Again, the strategy here was to look for the highest peak from the averaged waveform. The purpose of averaging the outcome of the SSM was to establish the performance of the SSM as a single-trial estimator; the mean SSM peak that is close to the EA peak reflects the accuracy of the individual single-trial outcome. Table 2 below summarizes the mean values of the P100's by EA and SSM for the sixteen subjects.

Table 2 - The mean P100's of the EA and SSM estimators for sixteen different subjects.

Subject	EA Method	SSM Method	Subject	EA Method	SSM Method
S1	99	100	S9	130	148
S2	100	100	S10	117	106
S3	119	120	S11	119	108
S4	128	132	S12	114	112
S5	99	118	S13	102	104
S6	107	105	S14	123	117
S7	108	109	S15	102	107
S8	107	115	S16	108	108

If the maximum allowable mean error (e_m) is set at ±5, SSM successfully estimated the P100's from subjects S1 ($e_m = 1$), S2 ($e_m = 0$), S3 ($e_m = 1$), S4 ($e_m = 4$), S6 ($e_m = 2$), S7 ($e_m = 1$), S12 ($e_m = 2$), S13 ($e_m = 2$), S15 ($e_m = 5$), and S16 ($e_m = 0$). On the other hand, SSM unsuccessfully estimated the intended peaks from subjects S5 ($e_m = 19$), S8 ($e_m = 8$), S9 ($e_m = 18$), S10 ($e_m = 11$), S11 ($e_m = 11$) and S14 ($e_m = 6$). Therefore with the given number of subjects, the success rate for SSM is at 62.5 %.

Illustrated in Figure 3 below is the SSM's extracted Pattern VEP for S3 from trial #1. It is to be noted that any peaks that occur below 90 ms are noise and are therefore ignored. Attention is given to any dominant (i.e., highest) peak(s) from 90 to 150 ms. From Figure 3, the highest peak produced by SSM is at 117 ms, which is close to 119 ms obtained by EA. On the other hand, the corrupted VEP (unprocessed raw signal) contains two dominant peaks at 110 and 116 ms, with the one at 110 ms being slightly higher. Therefore, SSM manages to suppress the peak at 110 ms so that the real P100 peak can be retrieved. In brief, the simulated and real data experiments exhibit the capability of the subspace technique in VEP estimation.

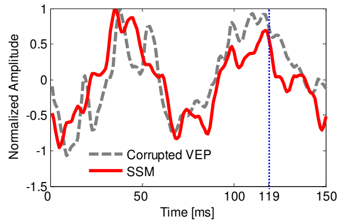

Figure 3 - The P100 of the third subject (S3) taken from trial # 1 (note: the P100 produced by the EA method is 119 ms).

4. CONCLUSIONS AND FUTURE WORK

A subspace method based on the eigendecomposition of the observed signal covariance matrix has been presented and tested to estimate the VEP's P100 peaks severely degraded by colored EEG noise. The results of the simulated and real patient data reveal that a subspace approach is a promising technique that can be further refined and applied in the real world as a single trial estimator of biomedical signals, which are currently extracted by means of multi-trial ensemble averaging.

Next, simulated and real human data involving the estimation of the VEP's P200 and P300 peaks are to be performed to further assess the capability of SSM. In order for the algorithm to function optimally, a suitable basis matrix for the eigendecomposition operation needs to be determined, so that both the signal and noise covariance matrices can be simultaneously and fully diagonalized.

ACKNOWLEDGMENT

We would like to thank Dr. Tara Mary George and Mr. Mohd Zawawi Zakaria of the Ophthalmology Department, Selayang Hospital, Kuala Lumpur for the VEP data.

REFERENCES

[1] L. Huszar, "Clinical Utility of Evoked Potential," eMedicine, April 18, 2006, retrieved May 5, 2006 from http://www.emedicine.com/neuro/topic69.htm.

[2] M. Zuki Yusoff, N. Kamel and A. Fadzil M Hani, "Single-Trial Extraction of Visual Evoked Potentials from the Brain," presented at the EUSIPCO 2008, Lausanne, Switzerland, Aug. 25-29, 2008.

[3] N. Kamel and M. Zuki Yusoff, "A Generalized Subspace Approach for Estimating Visual Evoked Potentials," in *Proc. IEEE EMBC'08,* Vancouver, Canada, Aug. 20-24, 2008, pp. 5208-5211.

[4] Y. Ephraim and H. L. Van Trees, "A Signal Subspace Approach for Speech Enhancement," IEEE Transaction on Speech and Audio Processing, vol. 3, no. 4, pp. 251-266, July 1995.

[5] A. Rezayee and S. Gazor, "An Adaptive KLT Approach for Speech Enhancement," IEEE Transactions on Speech and Audio Processing, vol.9, no.2, Feb. 2001.

[6] X. H. Yu, Z. Y. He and Y. S. Zhang, "Time-Varying Adaptive Filters for Evoked Potential Estimation," IEEE Transactions on Biomedical Engineering, vol. 41, no. 11, Nov. 1994.